Electronic Supplementary Material (ESI) for Energy & Environmental Science
This journal is © The Royal Society of Chemistry 2011

Supporting Information

Enhanced electrochemical properties in olivine lithium phosphate cathodes by Fe doping

Yong-Mook Kang[a ‡*], Yong-Il Kim[b ‡], Min-Wook Oh[c], Ri-Zhu Yin[d], Youngmin Lee[a], Dong-Wook Han[e], Hyuk-Sang Kwon[e], Jung Ho Kim[f], Ganpati Ramanath[g*]

[a] Division of Advanced Materials Eng., Kongju National University, Chungnam, Republic of Korea

[b] Korea Research Institute of Standards and Science, Yuseong, Daejeon, Republic of Korea

[c] Korea Electrotechnology Research Institute, 28-1 Seongju-dong, Changwon 641-120, Republic of Korea

[‖]Department of Chemistry, Yonsei University, Seoul 120-749, Republic of Korea

[d] Department of Materials Science & Engineering, Korea Advanced Institute of Science & Technology, 373-1, Guseong-dong, Yuseong-gu, Daejon 305-701, Republic of Korea

[e] Institute for Superconducting & Electronic Materials, University of Wollongong, NSW 2522, Australia

[f] Materials Sci. & Eng. Dept., Rensselaer Polytechnic Institute, 110 Eighth Street, Troy NY 12180, USA

[*] Corresponding authors: dake1234@kongju.ac (Yong-Mook Kang), Ramanath@rpi.edu (Ganpati Ramanath)

Experimental

(1) *Ab initio* calculation

Total-energy calculations and full structural optimization in this work were performed in a plane-wave basis set using the projector augmented-wave (PAW) method as implemented in the Vienna *ab initio* simulation package.[19] To assure the convergence of energy, a cut-off value of 500 eV was used. The size of the k mesh was chosen to be 6×10×11 to ensure that the total energy converges within 1 meV per the conventional unit cell. Total-energy minimization via lattice parameter optimization and atomic position relaxation was reduced to 0.02 eV/Å for each atom. Electron correlation within the *d* states significantly affects the electronic structure and energetic properties of the lithium transition metal phosphate. Hence, significant errors in the electronic structure are often reported from calculations based on the local density approximation (LDA) or generalized gradient approximation (GGA).[20] Considering on-site Coulomb interaction correction for the *d* states of the transition metals, the rotationally invariant GGA+U approach was used.[20] The self-consistently calculated U values of U = 6.05 eV and U = 4.71 eV were used for $LiCoPO_4$ and $LiFePO_4$, respectively. The value of J was 1 eV in both cases. The antiferromagnetic (AFM) spin configuration was primarily assumed in the calculation.

(2) Preparation of $LiCoPO_4$ and Fe-doped $LiCoPO_4$

$LiCoPO_4$, $LiCo_{0.95}Fe_{0.05}PO_4$, and $LiCoPO_4$/C and $LiCo_{0.9}Fe_{0.1}PO_4$/C compo-sites were prepared by solid state reaction of Li_3PO_4, $Fe_3(PO_4)2.8H_2O$, and $Co_3(PO_4)2.8H2O$, using high energy ball-milling and subsequent microwave heating. In the precursor mixing step, all precursors and 5 wt% acetylene black were put into a ball-milling jar at one time and then mixed by a vibrating type ball mill (SPEX8000 mixer/mill) under Ar atmosphere for 2 hours. The ball-milled mixture was pelletized and then set on a fixed point in a quartz crucible filled with activated carbon (Aldrich, 20-40 mesh). This quartz crucible was placed in a uniform heating region in a domestic microwave oven (750 W) and then irradiated with microwaves for 2-4 minutes to produce the crystallized $LiCoPO_4$/C or Fe-doped $LiCoPO_4$/C composites.

(3) Structural characterization

The phases of $LiCoPO_4$ and Fe-doped $LiCoPO_4$ were characterized by X-ray diffraction (XRD, Rigaku D/MAX-IIIC, 3kW) and high resolution neutron powder diffraction (HRPD). Several precise characterizations have been adopted to primarily

explain the change in $(PO_4)^{3-}$ polyhedra and Co oxidation states after Fe doping in $LiCoPO_4$. Synchrotron based X-ray absorption spectroscopy (XAS) is a very effective technique to investigate the structural and electronic properties of electrode materials. X-ray absorption near edge spectroscopy (XANES) and extended X-ray absorption fine-structure spectroscopy (EXAFS) can clearly reveal details about the local coordination, site symmetry, oxidation state, and bond characteristics around the element of interest. Hence, XANES and EXAFS data have been collected to investigate the neighboring structure around Co ions or Fe ions in $LiCoPO_4$ and Fe-doped $LiCoPO_4$. The X-ray absorption measurements, which included both XANES and EXAFS techniques, were performed on the BL7C1 beam line of the Pohang light source (PLS) with a ring current of 120-170 mA at 2.5 GeV. A Si(111) double-crystal monochromator was employed to monochromatize the X-ray photon energy. In order to investigate the nature of cation site occupancy in $LiCoPO_4$ and Fe-doped $LiCoPO_4$, Rietveld refinement was carried out on $LiCoPO_4$ and $LiCo_{0.95}Fe_{0.05}PO_4$. The initial crystal structural model of $LiCoPO_4$ was constructed with crystallographic data based on the monoclinic space group Pnma. Herein, structural refinement cycles included zero-point shift, scale factor, lattice parameters, and background parameters as variables. Following satisfactory matching of peak positions, atomic positions, thermal parameters, and peak profile parameters, including the peak asymmetry, were refined. α-Al_2O_3 (NIST SRM 676) powder was measured diffraction data

(3) Electrochemical Measurements

To fabricate electrodes, a mixture of 72 wt % of each active material and 20 wt % acetylene black were added to N-methyl-2-pyrrolidene (NMP) solution containing 8 wt % polyvinylidene fluoride (PVDF). This slurry was pasted onto an Al foil substrate and then dried at 120 ^{o}C for 6 h in a vacuum oven. After being dried, it was pressed and then punched into a disc shape 1.3 cm in diameter. Electrochemical properties of the prepared electrodes were evaluated using 2016 coin-type cells assembled in an argon-filled glove box. Li metal foil was used as the counter electrode and 1 M $LiPF_6$ dissolved in tetramethylene sulfone was adopted as the electrolyte, as it has strong resistance to oxidation even at high applied potential up to 5 V. The cells were charged and discharged galvanostatically between 3.5 and 5.2 V at 30 ^{o}C. Finally, open circuit voltage (OCV) vs. closed circuit voltage (CCV) testing over 3.5–5.2 V (vs. Li/Li^+) was chosen as another electrochemical measurement to investigate the changes in electrode resistance during Li^+ intercalation/de-intercalation.

Rietveld analysis of X-ray and neutron diffractograms from $LiCoPO_4$ show that the D model is a better description of the structure of our sample. The D-model assumes that both the 4a and 4c sites were fully occupied by either Li or Co, and the sum of their occupation probabilities for a given site equals unity. The converged weighted R-factor R_{wp} and goodness-of-fit indicator S (= R_{wp}/R_e) for the D-model (see Fig. S1 and Tables S1A-B) are slightly lower than those for the O-model indicating that the D-model is a better description. Specifically, in the D-model, the 4a site has a Co occupancy of 0.008 while the 4c site has a Li occupancy of 0.027. We note that R_{wp} and S are the most meaningful indicators of the adequacy of the structural model because minimization of these parameters directly correspond to lower differences between the experimental data and calculated values.

In the case of Fe-doped $LiCoPO_4$, Rietveld refinement results (Fig. S2 and Tables S2A-B) show a low occupancy of substitutional Fe in the 4*a* site (0.001) indicating that Fe prefers to substitute Co in the 4c site. Additionally, the antisite mixing of Li and Co is completely supressed. The R_{wp} and S values for both the O- and D-models are virtually identical, point to the same result.

.

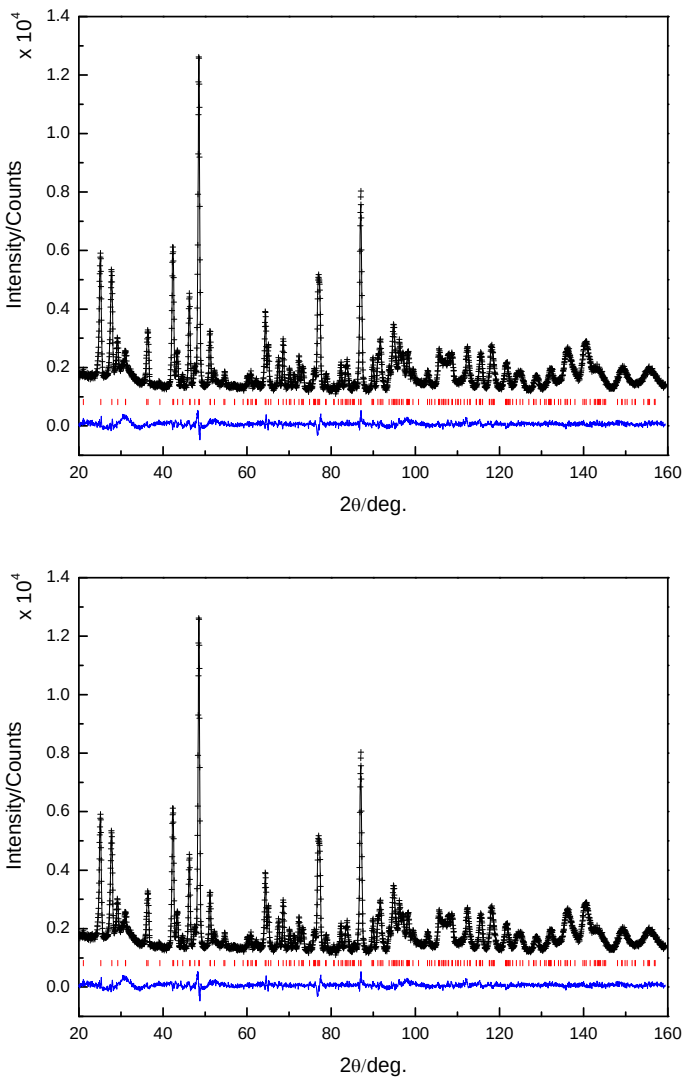

Fig. S1. Experimentally acquired (+) and Rietveld-calculated (solid line) X-ray diffractograms for $LiCoPO_4$ using the D-model (top) and the O-model (bottom). The difference between the experimental and calculated values is plotted below the diffractogram. The tick marks between the two curves indicate Bragg reflections. See Table S1 for detailed atomic positions, weighting factors and lattice parameters extracted by our Rietveld analyses.

Table S1. Structural parameters for $LiCoPO_4$ obtained from the Rietveld refinement of room-temperature neutron diffractograms using (A) the Disordered model and (B) the Ordered model. The symbol *g* is the occupation probability of a given element at a particular site. For the O-model all Li occupy *4a* sites and all Co occopy *4c* sites and $g_{Li} = g_{Co} = g_O = 1$. For the D-model, $g_{Li} + g_{Co}=1$ for each site. For both models, the structure is specified by the *Pnma* space group and $Z = 4$. The parenthetic numbers next to elements are site labels. For $LiCoPO_4$, Co(1) and Li(2) are antisite defects. The last digits of numbers after the decimal place enclosed in parentheses denote the estimated standard deviations of the last significant figure.

A. Disordered model

Atom	**Site**	***x* (Å)**	***y* (Å)**	***z* (Å)**	***g***	**$100*U_{iso}$ (Å^2)**
Li(1)	4*a*	0.0	0.0	0.0	0.992(10)	2.50(25)
Co(2)	4*a*	$= x_{Li(1)}$	$= y_{Li(1)}$	$= z_{Li(1)}$	0.008(10)	$= U_{iso}$(Li(1))
P	4*c*	0.0944(3)	1/4	0.4191(5)	1.0	0.24(5)
wO(1)	4*c*	0.0979(3)	1/4	0.7411(5)	1.0	0.73(6)
O(2)	4*c*	0.4546(2)	1/4	0.2037(6)	1.0	0.41(6)
O(3)	8*d*	0.1664(2)	0.0452(3)	0.2823(4)	1.0	0.75(4)
Co(1)	4*c*	0.2787(6)	1/4	0.9839(13)	0.973(6)	0.12(11)
Li(2)	4*c*	$= x_{Co(1)}$	$= y_{Co(1)}$	$= z_{Co(1)}$	0.027(6)	$= U_{iso}$(Co(1))

<u>*Lattice parameters:*</u> $a = 10.2131(3)$ Å $b = 5.9270(1)$ Å $c = 4.7061(1)$ Å $\alpha = \beta = \gamma = 90$ °
<u>*Weighted R factors:*</u> $R_{wp}= 3.89$ %, $R_p= 3.00$ %, $S = 1.68$

B. Ordered model

Atom	**Site**	***x* (Å)**	***y* (Å)**	***z* (Å)**	***g***	**$100*U_{iso}$ (Å^2)**
Li(1)	4*a*	0.0	0.0	0.0	1.0	2.50(25)
Co(1)	4*c*	0.2785(6)	1/4	0.9837(13)	1.0	0.42(11)
P	4*c*	0.0945(3)	1/4	0.4190(5)	1.0	0.25(5)
O(1)	4*c*	0.0978(3)	1/4	0.7412(5)	1.0	0.73(6)
O(2)	4*c*	0.4546(2)	1/4	0.2039(6)	1.0	0.41(6)
O(3)	8*d*	0.1664(2)	0.0453(3)	0.2822(4)	1.0	0.74(4)

<u>*Lattice parameters:*</u> $a = 10.2131(3)$ Å $b = 5.9270(2)$ Å $c = 4.7061(1)$ Å $\alpha = \beta = \gamma = 90$ °
<u>*Weighted R factors:*</u> $R_{wp}= 3.98$ %, $R_p= 3.32$ %, $S = 1.72$

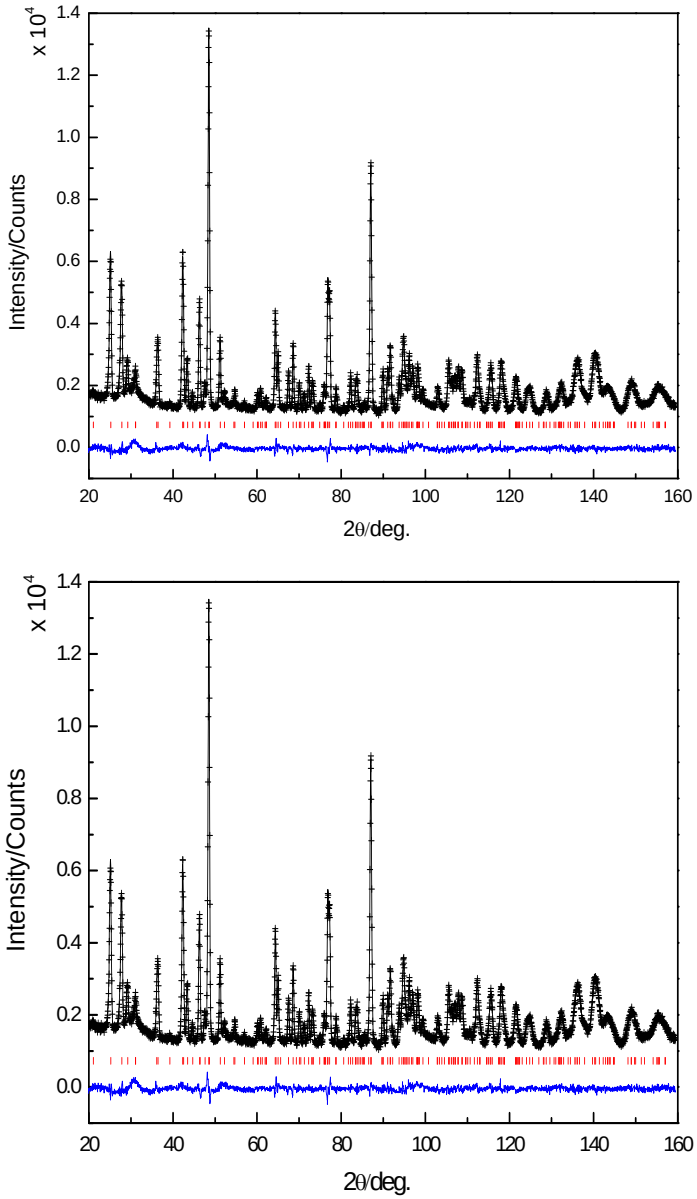

Fig. S2. Experimentally acquired (+) and Rietveld-calculated (solid line) X-ray diffractograms for $LiCo_{0.95}Fe_{0.05}PO_4$ using the D-model (top) and the O-model (bottom). The difference between the experimental and calculated values is plotted below the diffractogram. The tick marks between the two curves indicate Bragg reflections. See Table S1 for detailed atomic positions, weighting factors and lattice parameters extracted by our Rietveld analyses.

Table S2. Structural parameters for $LiCo_{0.95}Fe_{0.05}PO_4$ obtained from the Rietveld refinement of room-temperature neutron diffractograms using (A) the D-model and (B) the O-model. The symbol *g* is the occupation probability of a given element at a particular site. For the O-model all Li occupy *4a* sites and all Co occopy *4c* sites and $g_{Li} = g_{Co} = g_O = 1$. For the D-model, $g_{Li} + g_{Co}=1$ for each site. For both models, the structure is specified by the *Pnma* s pace group and $Z = 4$. The parenthetic labels next to elements are site labels. The last digits of numbers after the decimal place enclosed in parentheses denote the estimated standard deviations of the last significant figure.

A. Disordered

Atom	**Site**	***x* (Å)**	***y* (Å)**	***z* (Å)**	***g***	**100*U_{iso} (Å^2)**
Li(1)	4*a*	0.0	0.0	0.0	0.999(4)	1.98(18)
Fe(2)	4*a*	$= x_{Li(1)}$	$= y_{Li(1)}$	$= z_{Li(1)}$	0.001(4)	$= U_{iso}$(Li(1))
P	4*c*	0.0946(2)	1/4	0.4194(4)	1.0	0.33(4)
O(1)	4*c*	0.0982(2)	1/4	0.7413(4)	1.0	0.67(4)
O(2)	4*c*	0.4551(2)	1/4	0.2033(4)	1.0	0.47(5)
O(3)	8*d*	0.1662(2)	0.0451(2)	0.2817(3)	1.0	0.66(3)
Co(1)	4*c*	0.2785(4)	1/4	0.9806(9)	0.955(6)	0.23(7)
Fe(1)	4*c*	$= x_{Co(1)}$	$= y_{Co(1)}$	$= z_{Co(1)}$	0.045(6)	$= U_{iso}$ (Co(1))

Lattice parameters: $a = 10.2150(1)$ Å $b = 5.9320(1)$ Å $c = 4.7038(1)$ Å $\alpha = \beta = \gamma = 90$ °
Weighted R factors: $R_{wp}= 3.75$ %, $R_p= 2.92$ %, $S = 1.60$

B. Ordered

Atom	**Site**	***x* (Å)**	***y* (Å)**	***z* (Å)**	***g***	**100*U_{iso} (Å^2)**
Li(1)	4*a*	0.0	0.0	0.0	1.0	1.93(18)
Co(1)	4*c*	0.2785(4)	1/4	0.9807(9)	0.956(5)	0.18(12)
Fe(1)	4*c*	$= x_{Co(1)}$	$= y_{Co(1)}$	$= z_{Co(1)}$	0.046(5)	$= U_{iso}$(Co(1))
P	4*c*	0.0946(2)	1/4	0.4193(4)	1.0	0.32(4)
O(1)	4*c*	0.0981(3)	1/4	0.7415(4)	1.0	0.67(4)
O(2)	4*c*	0.4551(2)	1/4	0.2033(3)	1.0	0.47(5)
O(3)	8*d*	0.1662(2)	0.0450(2)	0.2816(3)	1.0	0.66(3)

Lattice parameters: $a = 10.2150(1)$ Å $b = 5.9320(1)$ Å $c = 4.7038(1)$ Å $\alpha = \beta = \gamma = 90$ °
Weighted R factors: $R_{wp}= 3.76$ %, $R_p= 2.92$ %, $S = 1.60$

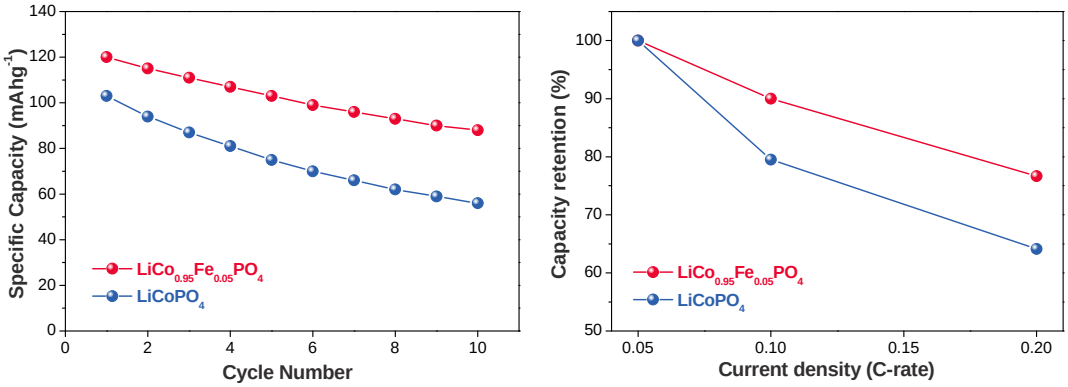

(a) (b)

Fig. S3. The comparison between $LiCoPO_4$ and $LiCo_{0.95}P_{0.05}O4$ in terms of (a) cycle life and (b) rate capability